Secondary Kinetic Isotope Effect on the Photoenolization of Triplet *O*-Methylanthrones. A Microcanonical Transition State Theory Calculation

Miquel Moreno* and José M. Lluch

Departament de Química. Universitat Autònoma de Barcelona, Edifici Cn, Campus de Bellaterra, 08193 Bellaterra (Barcelona), Spain

Received: April 18, 2007; In Final Form: July 13, 2007

The energy profile for the tautomerization reaction of 1,4-dimethylanthrone in the first triplet electronic state obtained through electronic calculations (B3LYP/ 6-31G(d)) is used to calculate the rate constants for the process at a wide range of energies using a modified RRKM microcanonical statistical formalism that takes into account tunneling. Through partial or total substitution of the hydrogen atoms of the methyl groups by deuterium atoms, it is possible to evaluate different primary and secondary kinetic isotope effects (KIE). These results can be compared with experimental data for these processes taking place in solid matrix at extremely low temperatures (4−50 K). Such a comparison allows us to conclude that the reaction is taking place at energies just slightly below (around 0.5 kcal/mol) the adiabatic potential energy barrier, a result that was previously found for other related molecules so that this mechanism may be extended to the photoenolization of other *o*-aryl methyl ketones. Analysis of the different factors contributing to the primary and secondary KIEs discloses that at energies not far below the adiabatic barrier, the tunneling effect is not the only factor that accounts for the large KIE but the differences in the energy level distribution upon isotopic substitution may be the predominant factor at a certain range of negative energies (this is especially so for the case of primary KIE). At positive energies (above the barrier) the levels factor is always the dominant factor in the total KIE.

1. Introduction

The study of chemical reactivity in electronically excited states is quite a complicated task both from experimental and theoretical aspects. Over the last 12 years, Garcia-Garibay's group has extensively studied the photoinduced hydrogen-atom transfer that takes place at ultralow temperatures (3−50 K) in different *o*-methyl aryl ketones.[1−8] From these studies, on the basis of phosphorescence lifetimes and total intensity measurements, it is now well-established that the more stable keto form of the molecule in the ground (singlet) electronic state (**^{1}K**) can be electronically excited up to a (singlet) excited electronic state. From there a rapid intersystem crossing leads to the lowest triplet electronic state (**^{3}K**). In this state the transfer of a hydrogen atom from the *o*-methyl group to the carbonyl oxygen can take place leading to the triplet enol tautomer **^{3}E**. After that, another intersystem crossing leads to the ground-state singlet enol **^{1}E** which can easily revert to the starting **^{1}K** structure through a back-hydrogen transfer process. This process competes with thermal (k_{TS}) and radiative (phosphorescence, k_P) decays of **^{3}K**. The different decay ways are illustrated in Figure 1 for the 1,4-dimethylanthrone (1,4-MAT).

Recently we have analyzed from a theoretical point of view the kinetics of the hydrogen-atom transfer in the lowest triplet state of several *o*-methyl aryl ketones.[9,10] Through the use of the well-known RRKM kinetic formalism, modified to take into consideration the possibility of tunneling of the transferring hydrogen, we found that the experimentally measured rate constants for 1,4-MAT when all the methyl-group hydrogens were deuterated were in accordance with the reaction taking place entirely by tunneling at energies shortly below the energy barrier.[9] As expected for a tunneling-dominated reaction, a curved Arrhenius plot was observed at the lowest temperatures, which, in our microcanonical treatment, corresponds to the lowest energies. Our results were also in accordance with the absence of phosphorescence observed for the original (nondeuterated) 1,4-MAT as the rate measured at the same energies was high enough ($\sim 10^8$ s^{-1}) to prevent phosphorescence to compete with triplet decay by hydrogen transfer (this fact poses an experimental lower limit of 10^6 s^{-1} to the H-atom transfer reaction). A second theoretical work was devoted to another member of the *o*-methyl aryl ketones family: 6,9-dimethylbenzosuberone.[10] In that case, the rate constants were clearly lower than the ones found for 1,4-MAT, so that now phosphorescence was confirmed to occur for both the original and deuterated molecules. Again, the results compared well with the ones from phosphorescence experiments measured by Garcia-Garibay and co-workers if the total energy lied just below the energy barrier. Now it was also possible to directly compare the obtained and measured primary kinetic isotope effects (KIE) for the deuterium substitution. The anomalous behavior of the KIE at the lowest end of the temperature range found in the experimental data was theoretically explained in terms of the total decay rate of the triplet state of 6,9-dimethylbenzosuberone being dominated by the phosphorescence and thermal decay rates at very low temperatures.[10]

In a more recent work, Garcia-Garibay and co-workers have obtained the isotopomer of 1,4-MAT with two deuterium and one hydrogen atom at each one of the two methyl groups and compared the rate constant of this molecule with the one with full methyl-hydrogen deuteration.[8] Assuming that phosphores-

* Corresponding author. Tel.:+34935812174; Fax: +34935812920. E-mail: miquel.moreno@uab.cat.

10.1021/jp0730040 CCC: $37.00
Published on Web 09/18/2007

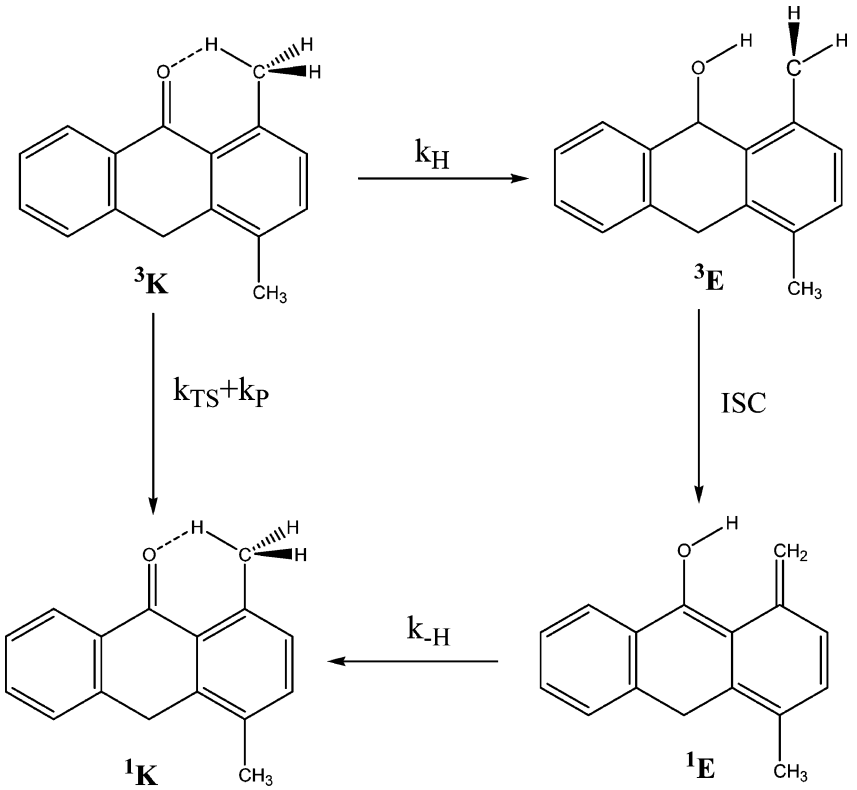

Figure 1. Different competing paths for the decay of the triplet 1,4-dimethylanthrone **^{3}K** back to the ground state.

cence measures can only be done when the atom transferred is a deuterium, they obtain again a curved Arrhenius plot with a limit rate constant of 2.2×10^4 s^{-1} as temperature approaches 0 K. Comparing this result with the one for the full-deuterated species, they are able to measure the α-secondary kinetic isotopic effect on 1,4-MAT. The obtained limit value of 2.4 is quite high for a secondary isotope effect and is also remarkable, as few experimentally secondary KIEs have been measured for hydrogen-transfer reactions in excited electronic states. In the same work[8] an attempt is made to explain this result by using a quite crude model of tunneling that considers a parabolic barrier with imaginary frequency $\nu^{\ddagger}$, but the so obtained rate constants are 2 orders of magnitude larger than those determined experimentally.

In this work we propose to apply our theoretical model, that combines quantum-chemical calculations and a statistical dynamic method based on the RRKM formalism, to analyze the secondary isotope effect on the hydrogen transfer reaction of triplet 1,4-dimethylanthrone. Up to now our methodology has performed well in the study of the primary isotope effects for the H-atom transfer in 1,4-dimethylanthrone and other *o*-methyl aryl ketones. As secondary effects are much less conspicuous, it will be interesting to see if our method is also capable of correctly dealing with such a difficult case. Within our theoretical model we will also be able to analyze on theoretical grounds the reasons behind the large secondary isotope effect on this reaction. Finally we will consider the possibility that the obtained conclusions might be generalized to the ubiquitous intramolecular hydrogen-transfer reactions in excited electronic states.

2. Theoretical Methods

2.1. Electronic Structure Methods. Density functional theory (DFT) methods have been used to obtain the stationary points for the hydrogen-atom transfer reaction and the harmonic frequencies to be used later on in the dynamic calculations. In particular we have considered the popular B3LYP hybrid density functional[11] with a double-ζ quality 6-31G(d) basis set, which includes a set of d-polarization functions on atoms other than hydrogens.[12] As calculations are carried out for the first triplet electronic state, the unrestricted version of the functional (sometimes called UB3LYP) is the one actually used.

Stationary points were located through the minimization procedure of Schlegel by using redundant internal coordinates.[13] The nature of the stationary points was checked through diagonalizing the energy second-derivatives matrix: No negative eigenvalues indicate a minimum on the potential energy surface whereas one negative eigenvalue is the signature of a transition-state structure. This calculation also provides the vibrational frequencies to be used in the dynamic method. It should be noted that this diagonalization has to be done for each isotopically substituted species. To verify the quality of the UB3LYP method, energies of the stationary points were recalculated with the unrestricted Hartree−Fock method and including the dynamical correlation with the Møller−Plesset perturbation theory up to the fourth order (MP4) taking in consideration all the double and quadruple excitations.[14] Again the 6-31G(d) basis set was used for these calculations.

All the calculations performed here have been done with the Gaussian 03 series of programs.[15]

2.2. Dynamic Method. The dynamic method used here is analogous to the one used for the study of 6,9-dimethylbenzosuberone so that just a brief outline is given here. Full details are to be found elsewhere.[10]

The microcanonical rate constant at a given energy E is evaluated using the expression:

$$k(E) = \frac{\sum_{E_{vib}} \rho^{\ddagger}(E_{vib}) \cdot P(E,E_{vib})}{h\rho_0(E)} \qquad (1)$$

where the summatory is taken over E_{vib}, the energy distributed along the transition-state vibrational modes. $\rho^{\ddagger}(E_{vib})$ is then the density of states for vibrational modes at the transition-state structure and $\rho_0(E)$ the density for the reactant molecule. These densities are obtained through a direct count method using the Beyer−Swinehart algorithm that gives an exact result for harmonic vibrations provided that the grain-size for the energy is significantly smaller than the lowest frequency considered.[16] In particular we have used a grain-size of 10 cm^{-1} which is smaller than the lowest frequencies of the reactant species (∼20 cm^{-1}). We have verified that using a smaller energy gap does not significantly affect the obtained results.

$P(E,E_{vib})$ in eq 1 is the transmission probability along the reaction coordinate. It is calculated using the semiclassical WKB approximation as:[17]

$$P(E,E_{vib}) = \begin{cases} 0 & E \le E_0 \\ \dfrac{1}{1+e^{2\theta(E)}} & E_0 \le E \le V^{\ddagger} + E_{vib} \\ 1 - P[2(V^{\ddagger} + E_{vib}) - E] & V^{\ddagger} + E_{vib} \le E \le 2\,(V^{\ddagger} + E_{vib}) - E_0 \\ 1 & 2(V^{\ddagger} + E_{vib}) - E_0 \le E \end{cases} \quad (2)$$

where E_0 is the energy of the ground vibrational state of the reactant minimum (assuming the reaction is exoergic), $V^{\ddagger}$ is the classical potential energy barrier, and $\theta(E)$ is the classical action integral through the barrier. The function used for the probability has been previously used in other schemes such as the semiclassical approximation to the transmission coefficient in the context of the generalized transition state theory.[18] It varies from 0 to 1 and includes also the nonclassical reflection for energies above the barrier. It is also to be noted that the final global expression used to obtain the rate constant is just the classical RRKM expression if the probability is given by:[19]

$$P(E,E_{vib}) = \begin{cases} 0 & E < V^{\ddagger} + E_{vib} \\ 1 & E \ge V^{\ddagger} + E_{vib} \end{cases} \quad (3)$$

It should be noted that this formalism does not account for rotation, so that the obtained rate constants are just for the case of a null total angular momentum ($J = 0$). In any case, for a large molecular system, such as the one considered here, it is not expected that rate constants and the kinetic isotope effect will be much affected by the neglect of the rotational degrees of freedom.

To end this section, it is important to bear in mind that our kinetic model is based on a simplified model and that there are many effects not included in our model that may be important. For instance, as the rate constant is obtained within the transition state theory, recrossing is not taken into account. However, at the very low temperature of the experiments (below 50 K), this factor is expected to be quite small. Another small correction that may be expected at the ultralow temperature limit is the inclusion of anharmonicities (the Beyer−Swinehart algorithm is based on a bath of harmonic oscillators). As the reaction occurs with a small amount of energy, the more significant corrections will probably come from the treatment of tunneling. For instance, it is well-known that the optimal tunneling trajectory tends to separate from the minimum energy path (corner-cutting).[18] Our treatment also does not consider quantum fluctuations around optimal trajectory. More sophisticated treatments have been proposed that take into account these corrections within a framework based on the generalized transition state theory[18] or calculating the transmission probability using the semiclassical instanton theory that finds the most rigorous tunneling path.[20,21] More recently,[22,23] a quantum transition-state theory also based on the instanton model (that also considers the quantum fluctuation effects) has been proposed to evaluate the KIE. In any case these quite sophisticated calculations cannot be applied to a system as large as the *o*-methylanthrones with a huge number (87) of vibrational degrees of freedom.

SCHEME 1

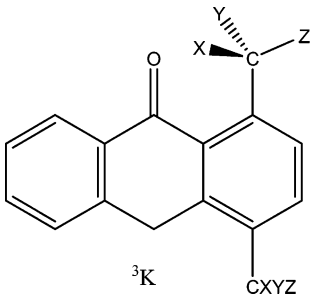

	X	Y	Z
MATH3	H	H	H
MATD2H	D	D	H
MATDHD	D	H	D
MATD3	D	D	D

Results and Discussion

In this work we analyze three different isotopomers of 1,4-dimethylanthrone: the perprotio one (without deuteration of the methyl hydrogens), the fully deuterated case, and the case with two deuteriums and one hydrogen in each methyl group. In the last case the atom to be transferred to the carbonyl group atom can be either a hydrogen or a deuterium. To name all the different cases we will use the criteria depicted in the Scheme 1 where the atom to be transferred is labeled as "Y". Given that X and Y positions are equivalent, we have studied two cases: MATD2H where the hydrogen cannot be transferred (this is the case experimentally studied) and the MATDHD case where a hydrogen atom is transferred. We have not considered the MATHDD case (equivalent to the MATDHD but with the deuterium transferring now), as the deuterium transfer cannot compete with the much faster hydrogen transfer process.

It should be noted that the isotopomers with just one deuterium at each methyl group, also studied in the experimental work,[8] have not been considered. In that case the decay rate is too fast to be experimentally measured, as hydrogen transfer is feasible for all the conformations. The same happens for the nondeuterated MATH3 species because the hydrogen atom transfer is too fast ($k_H > 10^6\ s^{-1}$) to allow for phosphorescence to compete with tautomerization. Given that the experiments are carried out in solid matrix at very low temperature, it can be safely assumed that the methyl-group rotation is frozen (at the time scale of the hydrogen-atom transfer). This explains why the monodeuterated isotopomers do not show phosphorescence: all the methyl conformations allow for a transfer of a hydrogen atom. It also gives account of the lower intensity observed for the phosphorescence spectra of the bideuterated case as compared with the fully deuterated compound (the relative intensities being close to the 1/3 statistical ratio).

The pure electronic calculations were previously presented.[9] At the UB3LYP/ 6-31G(d) level the high-energy barrier for the tautomerization in the ground singlet electronic state (43.11 kcal/mol) is largely lowered in the first triplet state (7.68 kcal/mol). We have tested these results by reevaluating the energy barrier in the triplet state using the more computational demanding MP4 method (see Theoretical Methods for details). At this high level the energy barrier in the triplet state is somewhat lowered (6.58 kcal/mol). In any case we have verified that correcting the

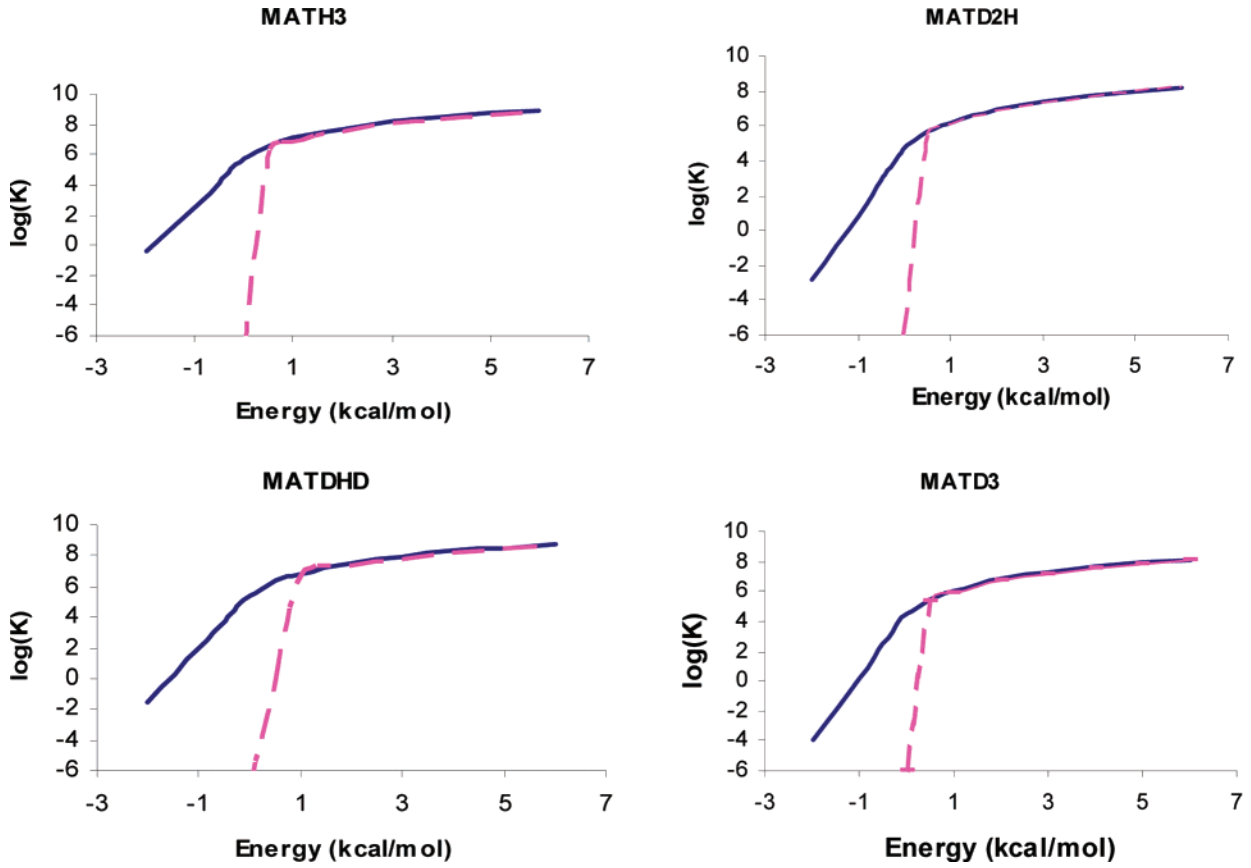

Figure 2. Logarithm of the microcanonical quantum rate constants (solid) and classical rate constants (dashed) for the different isotopomers of 1,4-dimethylanthrone. Molecules are labeled as indicated in Scheme 1.

energy profiles to take into account the MP4 results does not appreciably modify the kinetic results presented below so that in the following all the results are obtained within the UB3LYP/6-31G(d) energy profiles.

Figure 2 presents the hydrogen-transfer rate constants in ^{3}**K** obtained within our theoretical procedure as outlined in the previous section. We consider the four isotopomers of the scheme even though the MATH3 and MATD3 cases were already studied in our previous work.[9] However, in that work we used the classical density of states for the harmonic oscillator to evaluate the density of states so that direct comparison with the present ones could be somehow biased. In any case it is interesting to have the whole set of results in compact form. Since it is not possible to know the amount of energy the system still possesses when it emerges in the ^{3}**K** state, we have carried out rate constant calculations for a wide range of energies.

The energy in the plots of Figure 1 is given relative to the transition state structure including the zero-point vibrational energy so that it is different for each isotopomer. Therefore, a positive energy means an over the barrier process whereas at negative energies the only operative process is nuclear tunneling. In this way, the quantum and classical rates are quite different at negative energies, as the classical rate falls suddenly to zero at the top of the barrier whereas the quantum rate shows a much more smooth drop. In any case, it is noted that the slope for the diminution of the rate constant at lower energies is dramatically enhanced when tunneling comes into play so that at energies 1 kcal/mol below the barrier, the tautomerization reaction has an almost negligible value. It is also to be remarked that at positive energies both quantum and classical rate constants rapidly converge, indicating that when the classical over the barrier process is allowed, the tunneling plays a very minor role in the global rate. Of course, this result is partially biased by the RRKM formalism that implies a random distribution of the energy among all the vibrational modes. A treatment that took into account the actual dynamics of the energy transfer between the different degrees of freedom would probably show that tunneling is still important at slightly positive energies.

A direct comparison of the theoretical rates constants presented in Figure 2 with the ones coming from phosphorescence experiments, as given in Figure 1 of ref 8, presents an obvious problem as we are obtaining microcanonical rate constants (i.e., rate constants at a given energy) whereas the experimental data consists of the rate constants at different temperatures. Usually it is possible to obtain thermally averaged rate constants from constant energy rate constants by performing an integral over all the available energies at a given temperature:

$$k(T) = \int_0^\infty k(E) f(E,T) \mathrm{d}E \qquad (4)$$

where $f(E,T)$ is the energy distribution at temperature T. For a reaction taking place in the ground electronic state, it is customarily assumed that initially the system is at thermal equilibrium so that the energy distribution follows the classical Boltzmann distribution.

However, the Boltzmann distribution does not apply here because the reaction does not take place in the ground electronic state, and thermal equilibrium cannot be assumed in this context. If we recall the whole mechanism for the photoenolization of anthrones outlined in the introduction, the triplet state is accessed after excitation from the ground to an excited singlet electronic state that somehow relaxes until an intersystem crossing puts the system in the triplet state. Up to now, we do not have enough data of the energy profiles of the excited electronic states to

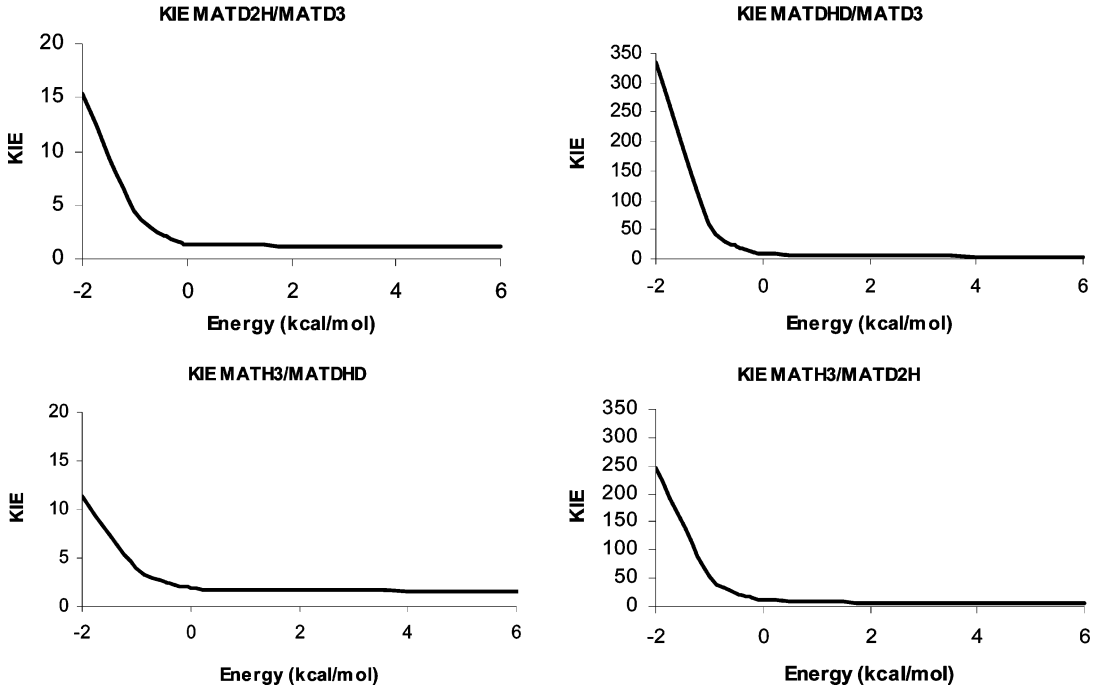

Figure 3. Kinetic isotope effects (KIE) for several pairs of isotopomers of 1,4-dimethylanthrone as a function of the energy.

exactly know at what energy the molecule will appear in the triplet state. Once in the triplet state, the molecule can vibrationally relax before the triplet decay processes (thermal, phosphorescence, and H-atom transfer) come into play. Given that experimentally the reaction is studied in a solid matrix at extremely low temperatures (below 50 K), it seems likely that vibrational relaxation will be quite slow. This is an important point given that if vibrational relaxation were fast enough, the triplet state would have time to become thermally equilibrated, but because of the high-energy barrier of 7.68 kcal/mol for the tautomerization reaction in the triplet state, thermally averaged $k(T)$ rate constant would give a value that is too small. We have previously noted that a higher computational level (MP4) lowered the barrier a little bit, but even a barrier as small as 1 kcal/mol would give rate constants that are too low at the experimental range of temperatures (3−50 K).

If we assume that the calculated microcanonical rate constants, as presented in Figure 2, are reasonable, we may have a hint of the energy (or the range of energies) the system has before it reacts. A point in favor of that possibility is that the measured rate constants for deuterium transfer reactions are around 10^4 s^{-1} whereas for hydrogen transfers the rate constant should be larger than 10^6 s^{-1}. Both values agree with our calculations if the tautomerization reaction takes place through tunneling at energies just slightly below the energy barrier. A similar conclusion was reached in our previous work on 6,9-dimethylbenzosuberone[10] so that it seems that this behavior is characteristic of *o*-methyl aryl ketones.

To obtain a more quantitative comparison of the behavior of the different isotopomers, Figure 3 depicts the kinetic isotope effect KIE of several pairs of isotopomers of 1,4-MAT. The KIE is defined as the rate constants quotient between the two different isotopomers, and it is expected to provide more reliable data, as some of the expected errors of the calculation (for instance the inaccurate barrier heights) will partially cancel out as they are in both sides of the division. As the more interesting energy zone is the negative one, we have just considered here the rate constants that take into account the nuclear tunneling.

The two graphics on the left of Figure 3 correspond to secondary KIEs. That is, both isotopomers differ only in atoms not directly involved in the transfer. Conversely, the two graphics on the right are for primary KIEs, as the transferring atom is different in the two involved isotopomers (in fact for the case in the bottom right, the KIE is both primary and secondary). Of course, primary KIEs are much larger than secondary ones, but purely secondary effects may give more insights into the mechanism of the reaction, as they indicate to what extent the reaction involves motions of atoms not directly involved in the rearrangement process.[24]

The more interesting case to analyze is the one depicted in the top left of Figure 3. It gives the secondary KIE between the bideuterated and fully deuterated species when the transferring atom is a deuterium and is the only case with known experimental quantitative measures by Garcia-Garibay and coworkers[8] An Arrhenius plot of the measured rates constants for MATD2H and MATD3 gives a KIE limit of ∼2.4 as the temperature approaches 0 K. They do not give the actual data of the KIE at different temperatures but analysis of Figure 1 of ref 8 allows us to estimate the KIE at ∼50 K (the highest temperature where both rate constants are provided) as being around 1.4. Within our theoretical model, a KIE of 2.4 is found at an energy 0.5 kcal/mol below the barrier whereas the 1.4 value is reached just 0.1 kcal/mol below the energy barrier. As the energy takes positive values, the KIE rapidly stabilizes at a value of ∼1.2 though it keeps on a very slight decrease as energy increases. The limit of the KIE at very high energies can be evaluated using the classical approximation to the RRKM theory:[25]

$$k(E) = A\left(\frac{E - V^{\ddagger}}{E}\right)^{s-1} \tag{5}$$

where s is the total number of vibrational degrees of freedom, $V^{\ddagger}$ is the potential energy barrier, and A is the frequency factor:

$$A = \frac{\prod_{i=1}^{s} \nu_i}{\prod_{i=1}^{s-1} \nu_i^{\ddagger}} \tag{6}$$

where the frequencies are given in s^{-1}. At sufficiently high energies the rate constant is equal to the frequency factor so that the limit KIE can be obtained through division of the productories of frequencies for both isotopomers. For the MATD2H/MATD3 case, this leads to a value of 1.01 so that the secondary kinetic effect almost vanishes at energies clearly above the barrier.

The plot on the top right of Figure 3 also gives the KIE of the bideuterated versus fully deuterated 1,4-MAT, but in this case the KIE is primary, as the transferring atom for the MATDHD isotopomer is a hydrogen. Of course, this leads to a much higher KIE that reaches values of 335.4 when the energy is 2 kcal/mol below the barrier but, again, rapidly diminishes as the total energy matches the energy barrier so that 1 kcal/mol above the barrier the KIE is just 5.37 and 4.01 at 5 kcal/mol. The quotient of frequency factors now gives a larger value of 1.35 which is the expected limit of the KIE at very high energies. It should be noted that this value roughly coincides with the square root of the quotient of the reduced masses corresponding to the imaginary frequency of the transition-state structure which is 1.4 within our frequency calculation, and this factor can also be directly attributed to the differences of masses between hydrogen and deuterium ($\sqrt{2} = 1.4$). The same quotient of frequency factors for the previous secondary KIE gives a value of 1.01 (as here in both cases a deuterium is the transferring atom), thus confirming that the limit KIE just comes from a mass factor of the different transferring atom. In this case there is no experimental measure of the KIE for the MATDHD/MATD3 case as hydrogen transfer is too fast to allow for phosphorescence to compete with tautomerization. As already explained, this poses a lower limit to the rate constant of MATDHD of 10^6 s^{-1}, and so the KIE has to be higher than ~100 now. Again this fact points to a tunneling reaction with energies not far below the barrier.

The other two KIEs depicted in Figure 3 (bottom) correspond to comparison of the original (nondeuterated) MATH3 species and the bideuterated MATD2H / MATDHD case. On the left, the KIE corresponds to a purely secondary effect (MATH3/MATDHD) whereas both primary and secondary KIE are present in the MATH3/MATD2H comparison on the right. Again, these KIEs are not available from an experimental point of view, as the MATH3 case is too fast to allow for phosphorescence quantitative measures. In any case, both graphics parallel the ones on top of Figure 3 so that no new discussion is needed for these cases. Globally, the KIEs are now slightly lower than the previous ones (in special in the negative energy region governed by tunneling). This is somehow unexpected, as the two isotopomers are now differing in two deuterium atoms whereas in the previous comparison the difference was just one deuterium atom. In any case it is clear that the effects of successive deuteration are not additive and that the full deuteration of the methyl groups leads to an additional slowing down of the tautomerization rate constant.

Up to now we have been able to explain the isotope effects on the tautomerization rates of 1,4-MAT using pure theoretical data. Our theoretical procedure, that does not take into account any empirical parameter, can also be used to gain insight to the molecular reasons behind the different kinetic isotope effects. To this aim let us recall the expression used to calculate the rate constant (eq 1) which shows that the rate constant at a given energy depends on different terms: the number of states at the transition-state structure multiplied by the probability of the transfer (in the numerator) and the density of states for the reactant (in the denominator). Using subscripts A and B to denote two different isotopomers, KIE(A/B) can be factorized in two terms as:

$$\mathrm{KIE}(A/B) = \frac{\sum_{E_{\mathrm{vib}}} \rho_A^{\ddagger}(E_{\mathrm{vib}}) P(E_{\mathrm{vib}})}{\sum_{E_{\mathrm{vib}}} \rho_B^{\ddagger}(E_{\mathrm{vib}}) P(E_{\mathrm{vib}})} \times \frac{\rho_{0,B}}{\rho_{0,A}} \tag{7}$$

where dependence on the total energies have been omitted for clarity. The first fraction corresponds to the numerator and depends both on the density of states at the transition-state structure and the reaction probability (i.e., tunneling). It would be interesting to have a direct measure of the tunneling factor alone. We can obtain such a measure by dividing each summatory term by the same summatory of states withdrawing the transmission probabilities. This way we have:

$$\mathrm{KIE}(A/B) = \frac{(\sum_{E_{\mathrm{vib}}} \rho_A^{\ddagger}(E_{\mathrm{vib}}) \cdot P(E_{\mathrm{vib}}))/(\sum_{E_{\mathrm{vib}}} \rho_A^{\ddagger}(E_{\mathrm{vib}}))}{(\sum_{E_{\mathrm{vib}}} \rho_B^{\ddagger}(E_{\mathrm{vib}}) \cdot P(E_{\mathrm{vib}}))/(\sum_{E_{\mathrm{vib}}} \rho_B^{\ddagger}(E_{\mathrm{vib}}))} \times \frac{\sum_{E_{\mathrm{vib}}} \rho_A^{\ddagger}(E_{\mathrm{vib}})}{\sum_{E_{\mathrm{vib}}} \rho_B^{\ddagger}(E_{\mathrm{vib}})} \times \frac{\rho_{0,B}}{\rho_{0,A}} \tag{8}$$

Now the first fraction can be fully ascribed to the transmission probability ($\mathrm{KIE}_{tun}(A/B)$) whereas the other two terms give the contribution to the KIE that comes from differences in the energy level distribution of both isotopomers ($\mathrm{KIE}_{lev}(A/B)$) so that we can now separately analyze both factors.

Table 1 gives these two factors for the kinetic isotope effect between the MATD2H and MATD3 molecules (secondary KIE) and the analogue MATDHD/MATD3 (primary KIE) case. The other two KIEs analyzed in Figure 3 are not included in the table, as results are not significantly different. We consider a wide range of energies from −2 to 5 kcal/mol (remember that the energy is given relative to the energy barrier for the tautomerization reaction taking into account the zero point energies).

Not surprisingly, analysis of the tunneling contributions to the KIE show that they quickly approach 1, as the energy is over the barrier (positive values). This is true for both the primary and secondary KIE. It was also expected that they were larger in the case of primary isotopic substitution. As for the level contributions to the KIE, they are almost constant along the whole energy range for the secondary case (third column in Table 1) whereas they are larger but notably energy-dependent for the primary KIE (sixth column in Table 1).

Let us now pay special attention to the $E = -0.5$ kcal/mol case, as it is around this energy, as previously discussed, that the experimental measurements coincide with the calculated values. It is noted that the secondary KIE is dominated by the tunneling factor (2.01). This indicates that the nontransferred

TABLE 1: Tunneling and Level Contributions to the Total Kinetic Isotope Effect (KIE) for Two Different Pairs of Isotopomers[a]

	KIE D2H/D3 (secondary)			KIE DHD/D3 (primary)		
energy (kcal/ mol)	KIE_{tun}	KIE_{lev}	KIE_{tot}[b]	KIE_{tun}	KIE_{lev}	KIE_{tot}[b]
-2.0	12.65	1.22	15.43	40.65	8.78	356.91
-1.0	3.68	1.21	4.45	7.18	6.97	50.04
-0.5	2.01	1.18	2.37	2.89	6.39	18.47
0.0	1.16	1.18	1.37	1.25	5.94	7.42
0.5	1.08	1.16	1.25	1.11	5.57	6.18
2.0	1.05	1.15	1.21	1.07	4.74	5.07
5.0	1.03	1.15	1.18	1.07	3.81	4.08

[a] Molecules are labeled as indicated in Scheme 1. [b] The total KIE is the Product of Both Terms (see text for details).

hydrogen or deuterium atoms bound to the methyl group are, nevertheless, largely contributing to the global reaction path. This comes, of course, from the fact that the methyl group of the keto tautomer has to rearrange into a methylene group in the enol product (see Figure 1). Within our theoretical method this fact is clearly reflected in the total length of the reaction path that goes from the keto to the enol tautomer (needed to evaluate the transmission probability through the semiclassical WKB method). The total path length of 8.56 Å·$uma^{1/2}$ for the MATD3 species is notably larger than the 8.01 Å·$uma^{1/2}$ value calculated for the MATD2H case. Of course, a much smaller value comes out for the MATDHD case where the transferring atom is a hydrogen atom (7.84 Å·$uma^{1/2}$), and this accounts for the higher contribution to the tunneling KIE for the primary case. Finally, if we compare this value with the MATH3 case (7.55 Å·$uma^{1/2}$) we obtain additional proof of the importance of secondary isotopic substitution in the total length of the tautomerization reaction.

As for the primary effect, figures in Table 1 give a quite surprising result, as at the same total energy of −0.5 kcal/mol, the tunneling contribution to the KIE is noticeably lower than the corresponding level contribution (2.89 vs 6.39). As the tunneling KIE rapidly increases at lower energies, it becomes the dominant term for the rest of negative energies. Nevertheless, results in Table 1 alert against just considering the different tunneling rates of hydrogen and deuterium to evaluate the kinetic isotope effect at energies slightly below the potential energy barrier.

Conclusions

In this paper we have used electronic structure calculations to obtain the energy profile for the tautomerization reaction of 1.4-dimethylanthrone in the first triplet electronic state. Given that the remaining energy of the molecule is not known when it reaches the triplet state (through a process that involves electronic excitation, vibrational relaxation, and intersystem crossing), we have used a microcanonical RRKM formalism modified to take into account tunneling to evaluate the rate constant for a wide range of energies. Our results show that the rate constant rapidly goes to zero at energies below the adiabatic barrier even if tunneling is present. This is so because the whole reaction path does not consist only on the motion of the transferring hydrogen atom but includes reorganization of the rest of the molecule (the other hydrogens of the methyl group must also move and the carbon skeleton rearrange a little bit). This explains the large secondary kinetic isotope effect (KIE) measured for these systems when the hydrogen atoms of the methyl groups are partially substituted by deuterium atoms.

Agreement with the experimental secondary KIE at very low temperature (2.4) is found for energies slightly below the adiabatic barrier. As explained in Theoretical Methods, our methodology presents some limitations so that we cannot give quantitative data, but, as seen in Figure 2, the calculated rate constants, which vary quite smoothly above the energy barrier, sharply fall as energy goes below the barrier. Within 1 kcal/mol the rate constant drops by 5 orders of magnitude so that we believe that this is the range of energies accessed by the molecule. Additionally, because the time scale of the process is on the order of 10^{-4} to 10^{-6} s, it could be expected that intermolecular vibrational redistribution is faster so that the reaction would take place in a thermally equilibrated triplet state. However, the transfer rates rapidly go to 0 at energies below the adiabatic barrier (7.68 kcal/mol). In this particular case, the lack of vibrational relaxation can be ascribed to the experimental setup where the molecule is confined in a solid matrix at extremely low temperature (4−50 K).

Our theoretical method also allows for an analysis of the different factors contributing to the primary and secondary KIEs. In this way, it has been shown that at energies not far below the adiabatic barrier, the tunneling effect is not the only factor that accounts for the large KIE but the differences in the energy level distribution upon isotopic substitution may be the predominant factor at a certain range of negative energies (this is especially so for the case of primary KIE). At positive energies (above the barrier), the levels factor is always the dominant factor in the total KIE.

As a whole, the results presented here, together with the ones previously published using a similar methodology (refs 9 and 10), provide a global explanation for the primary and secondary KIE on the photoenolization of different *o*-methyl aryl ketones in solid glass at extremely low temperatures so that it can be concluded that all these processes are taking place at energies just slightly below the adiabatic potential energy barrier.

Acknowledgment. The authors are grateful for financial support from the "Ministerio de Educación y Ciencia" and the "Fondo Europeo de Desarrollo Regional" through project CTQ2005-07115/BQU, and from the "Generalitat de Catalunya" (2005SGR00400).

References and Notes

(1) Garcia-Garibay, M. A.; Gamarnik, A.; Pang, L.; Jenks, W. S. *J. Am. Chem. Soc.* **1994**, *116*, 12095.

(2) Garcia-Garibay, M. A.; Gamarnik, A.; Bise, R.; Pang, L.; Jenks, W. S. *J. Am. Chem. Soc.* **1995**, *117*, 10264.

(3) Johnson, B. A.; Gamarnik, A.; Garcia-Garibay, M. A. *J. Phys. Chem.* **1996**, *100*, 4697.

(4) Gamarnik, A.; Johnson, B. A.; Garcia-Garibay, M. A. *J. Phys. Chem. A* **1998**, *102*, 5491.

(5) Johnson, B. A.; Garcia-Garibay, M. A. *J. Am. Chem. Soc.* **1999**, *121*, 8114.

(6) Johnson, B. A.; Hu, Y.; Houk, K. N.; Garcia-Garibay, M. A. *J. Am. Chem. Soc.* **2001**, *123*, 6491.

(7) Johnson, B. A.; Kleinman, M. H.; Turro, N. J.; Garcia-Garibay, M. A. *J. Org. Chem.* **2002**, *67*, 6944.

(8) Campos, L. M.; Warrier, M. V.; Peterfy, K.; Houk, K. N.; Garcia-Garibay, M. A. *J. Am. Chem. Soc*. **2005**, *127*, 10178.

(9) Casadesús, R.; Moreno, M.; Lluch, J. M. *J. Phys. Chem. A* **2004**, *108*, 4536.

(10) Casadesús, R.; Moreno, M.; Lluch, J. M. *Chem. Phys*. **2006**, *328*, 410.

(11) (a) Lee, C.; Yang, W.; Parr, R. G. *Phys. Rev. B* **1988**, *37*, 785. (b) Becke, A. D. *J. Chem. Phys.* **1993**, *98*, 5648.

(12) Francl, M. M.; Pietro, W. J.; Hehre, W. J.; Binkley, J. S.; Gordon, M. S.; DeFrees, D. J.; Pople, J. A. *J. Chem. Phys.* **1982**, *77*, 3654.

(13) Peng, C.; Ayala, P. Y.; Schlegel, H. B.; Frisch, M. J. *J. Comput. Chem.* **1996**, *17*, 49.

(14) Krishnan, R.; Pople, J. A. *Int. J. Quantum Chem*. **1978**, *14*, 91.

(15) Gaussian 03, Revision C.02, Frisch, M. J.; Trucks, G. W.; Schlegel, H. B.; Scuseria, G. E.; Robb, M. A.; Cheeseman, J. R.; Montgomery, Jr., J. A.; Vreven, T.; Kudin, K. N.; Burant, J. C.; Millam, J. M.; Iyengar, S. S.; Tomasi, J.; Barone, V.; Mennucci, B.; Cossi, M.; Scalmani, G.; Rega, N.; Petersson, G. A.; Nakatsuji, H.; Hada, M.; Ehara, M.; Toyota, K.; Fukuda, R.; Hasegawa, J.; Ishida, M.; Nakajima, T.; Honda, Y.; Kitao, O.; Nakai, H.; Klene, M.; Li, X.; Knox, J. E.; Hratchian, H. P.; Cross, J. B.; Bakken, V.; Adamo, C.; Jaramillo, J.; Gomperts, R.; Stratmann, R. E.; Yazyev, O.; Austin, A. J.; Cammi, R.; Pomelli, C.; Ochterski, J. W.; Ayala, P. Y.; Morokuma, K.; Voth, G. A.; Salvador, P.; Dannenberg, J. J.; Zakrzewski, V. G.; Dapprich, S.; Daniels, A. D.; Strain, M. C.; Farkas, O.; Malick, D. K.; Rabuck, A. D.; Raghavachari, K.; Foresman, J. B.; Ortiz, J. V.; Cui, Q.; Baboul, A. G.; Clifford, S.; Cioslowski, J.; Stefanov, B. B.; Liu, G.; Liashenko, A.; Piskorz, P.; Komaromi, I.; Martin, R. L.; Fox, D. J.; Keith, T.; Al-Laham, M. A.; Peng, C. Y.; Nanayakkara, A.; Challacombe, M.; Gill, P. M. W.; Johnson, B.; Chen, W.; Wong, M. W.; Gonzalez, C.; Pople, J. A.; Gaussian, Inc., Wallingford CT, 2004.

(16) Beyer, T.; Swinehart, D. F. *Commun. ACM* **1973**, *16*, 379.

(17) Bell, R. P. *The Tunnel Effect in Chemistry*; Chapman and Hall: New York, 1980.

(18) Truhlar, D. G; Isaacson, A. D.; Garrett, B. C. In *Theory of Chemical Reaction Dynamics*; Baer, M., Ed.; CRC Press: Boca Raton, FL, 1985; pp 65−137.

(19) Miller, W. H. *J. Am. Chem. Soc.* **1979**, *101*, 6810.

(20) Miller, W. H. *J. Chem. Phys*. **1975**, *62*, 1899.

(21) Smedarchina, Z.; Siebrand, W.; Fernández-Ramos, A.; Cui, Q. *J. Am. Chem. Soc*. **2003**, *125*, 243.

(22) Miller, W. H.; Zhao, Y.; Ceotto, M.; Yang, S. *J. Chem. Phys*. **2003**, *119*, 1329.

(23) Vaníček, J.; Miller, W. H.; Castillo, J. F.; Aoiz, F. J. *J. Chem. Phys*. **2005**, *123*, 054108.

(24) (a) *Isotope Effects in Chemical Reactions*; Collins, C. J.; Bowman, N. S., Eds.; Van Nostrand Reinhold: New York, 1970. (b) Melander, L.; Saunders, W. H., Jr. *Reaction Rates of Isotopic Molecules*; Wiley: New York, 1986.

(25) (a) Robinson, P. J.; Holbrook, K. A. *Unimolecular Reactions*; Wiley: New York, 1972. (b) Forst, W. *Theory of Unimolecular Reactions*; Academic Press: New York, 1973.